

3D Porous Ni/NiO_x as a bifunctional oxygen electrocatalyst derived from Freeze dried Ni(OH)₂

Yuta Shudo,^a Masahiro Fukuda,^a Md. Saidul Islam,^{a, b} Keita Kuroiwa,^c Yoshihiro Sekine,^a Mohammad Razaul Karim,^{d, e} and Shinya Hayami ^{*a, b}

- a. *Department of Chemistry, Graduate School of Science and Technology, Kumamoto University, 2-39-1 Kurokami, Chuo-ku, Kumamoto 860-8555, Japan.*
- b. *Institute of Industrial Nanomaterials (IINa), Kumamoto University, 2-39-1 Kurokami, Chuo-ku, Kumamoto 860-8555, Japan*
- c. *Department of Nanoscience, Faculty of Engineering, Sojo University, 4-22-1 Ikeda, Nishi-ku, Kumamoto 860-0082, Japan*
- d. *Department of Chemistry, School of physical Science, Shahjalal University of Science and Technology, Sylhet-3114, Bangladesh*
- e. *Department of Chemistry, King Abdulaziz University, Jeddah 21589, Saudi Arabia*

This PDF file includes:

Calculation of Tafel slope and Turnover Frequency (TOF) for OER.

Calculation of the Koutechy-Levich (K-L) plot for OER.

Calculation of the hydrogen peroxide yield on ORR.

Figure S1. The SEM image of Freeze-dried Ni(OH)₂

Figure S2. XPS survey spectrum of freeze-dried Ni/NiO_x.

Figure S3. HAADF-STM-EDS spectra of the freeze-dried Ni/NiO_x.

Figure S4. CV of a) ordinary Ni/NiO_x, b) freeze-dried Ni/NiO_x, c) freeze-dried Ni(OH)₂ and d) freeze-dried NiO collected at different scan rate in 1.0 M KOH solution. e) Calculated double-layer capacitance (C_{dl}) each sample.

Figure S5. The OER curves of Freeze-dried Ni/NiO_x between 1st and 100th.

Figure S6. The chronoamperometric response of freeze-dried Ni/NiO_x at 1.5V

Figure S7. The OER curves of Freeze-dried Ni/NiO_x after measurement.

Figure S8. XPS spectra of Freeze-dried Ni/NiO_x after 100 scans.

Figure S9. The CV measurement of freeze-dried Ni/NiO_x under N₂ or O₂.

Figure S10. The yield of hydrogen peroxide on the ring electrode.

Figure S11. LSV curves for OER and ORR to evaluate ΔE .

Table S1. Comparison of the OER and ORR activity of freeze-dried Ni/NiO_x with those of Ni based products in reference.

Calculation of Tafel slope and Turnover Frequency (TOF) for OER. The Tafel plot is calculated by following equation:

$$\eta = a + b \times \log i$$

Where η is the over potential ($\eta = E_{RHE} - 1.23$), a is y-intercept, b is the Tafel slop, and i (mA / cm²) is the current density.

The TOF:

$$TOF = j \times A / (4 \times F \times n)$$

Where j is the current density, A is the surface area of the RDE, F is Faraday's constant (96485 C mol⁻¹), and n is the moles of sample on the RDE.

Calculation of the Koutechy-Levich (K-L) plot for OER. The number of electron transfer for ORR can be attributed by the K-L equation:

$$i^{-1} = i_k^{-1} + \left(0.62 \times n \times F \times A \times D_0^{2/3} \times \omega^{1/2} \times \nu^{-1/6} \times C_{O_2}\right)^{-1}$$

$$i^{-1} = i_k^{-1} + B^{-1} \times \omega^{-1/2}$$

$$B = 0.62 \times n \times F \times A \times D_0^{2/3} \times \nu^{-1/6} \times C_{O_2}$$

Where i_k is the kinetic current, and ω is the rotating rate of RRDE. B^{-1} , based on the Levich equation, is attributed to K-L slope. Where n is the number or electron transfer for ORR, F is Faraday's constant (96485 C mol⁻¹), A is Surface area, D_0 is the diffusion coefficient of Oxygen (1.9×10^{-5} cm² s⁻¹), ν is kinematic viscosity (0.01 cm² s⁻¹), C_{O_2} is the bulk concentration of O₂ (1.2×10^{-6}).

ω

Calculation of the hydrogen peroxide yield on ORR. The hydrogen peroxide yield (%) and the electron transfer number were determined by RRDE and follow equation.

$$H_2O_2 (\%) = 2 \times 100 \times \frac{I_r / N}{I_d + I_r / N}$$

$$n = \frac{4 \times I_d}{I_d + I_r / N}$$

Where I_r is current density of ring electrode, I_d is current density of disk electrode, N is

current efficiency of the ring electrode ($N=0.4$).

Cyclic voltammetry is performed with various scan rating (0.1, 0.08, 0.05, 0.01, 0.005 V/s).

For Linear sweep voltammetry (LSV) of OER, electrode is measured

BET Surface area measurement

Surface area measurement according to Brunauer, Emmett and Teller (BET) is equivalent to determining the amount of gas required to form a monomolecular or "monolayer" covering of gas on the solid substrate. Knowing the cross-section and number of gas molecules that make up the monolayer, the surface area of that substrate can easily be calculated.

The relevant mathematical formulation for B.E.T. equation is

$$\frac{1}{V(P_0/P-1)} = \frac{1}{(V_m C) + ((C-1))} \frac{P}{P_0}$$

where V is the total volume of gas adsorbed at the measured pressure P ; V_m is the volume required to cover the solid surface by monomolecular gas layer; P_0 is the saturating pressure of the gas at the adsorption temperature and C is a constant. By taking the ' $1/(V(P_0/P-1))$ ' as the ordinate and P/P_0 as the abscissa, a straight line of slope $(C - 1)/(V_m C)$ is obtained, with the intercept at the origin being $1/V_m C$.

To calculate these values, the BET equation is plotted as an adsorption isotherm typically at a relative pressure (P/P_0) between 0.05-0.30. In this range it forms a straight line. Sample does not produce a linear adsorption isotherm over the standard BET range ($P/P_0 = 0.05-0.3$). In particular, non-linearity is often obtained at P/P_0 values below 0.05 and after 0.3.

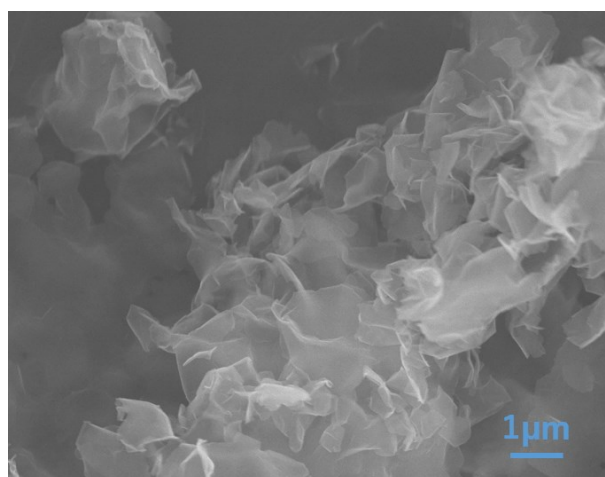


Fig. S1 The SEM image of Freeze-dried Ni(OH)₂

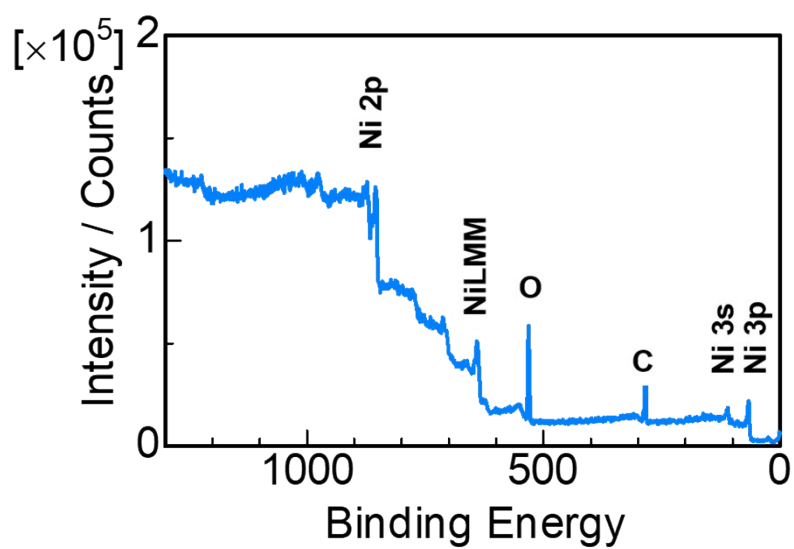


Fig. S2 XPS survey spectrum of freeze-dried Ni/NiO_x. Elemental composition of Ni/NiO_x includes Nickel (20.0%) and Oxygen (66.7%).

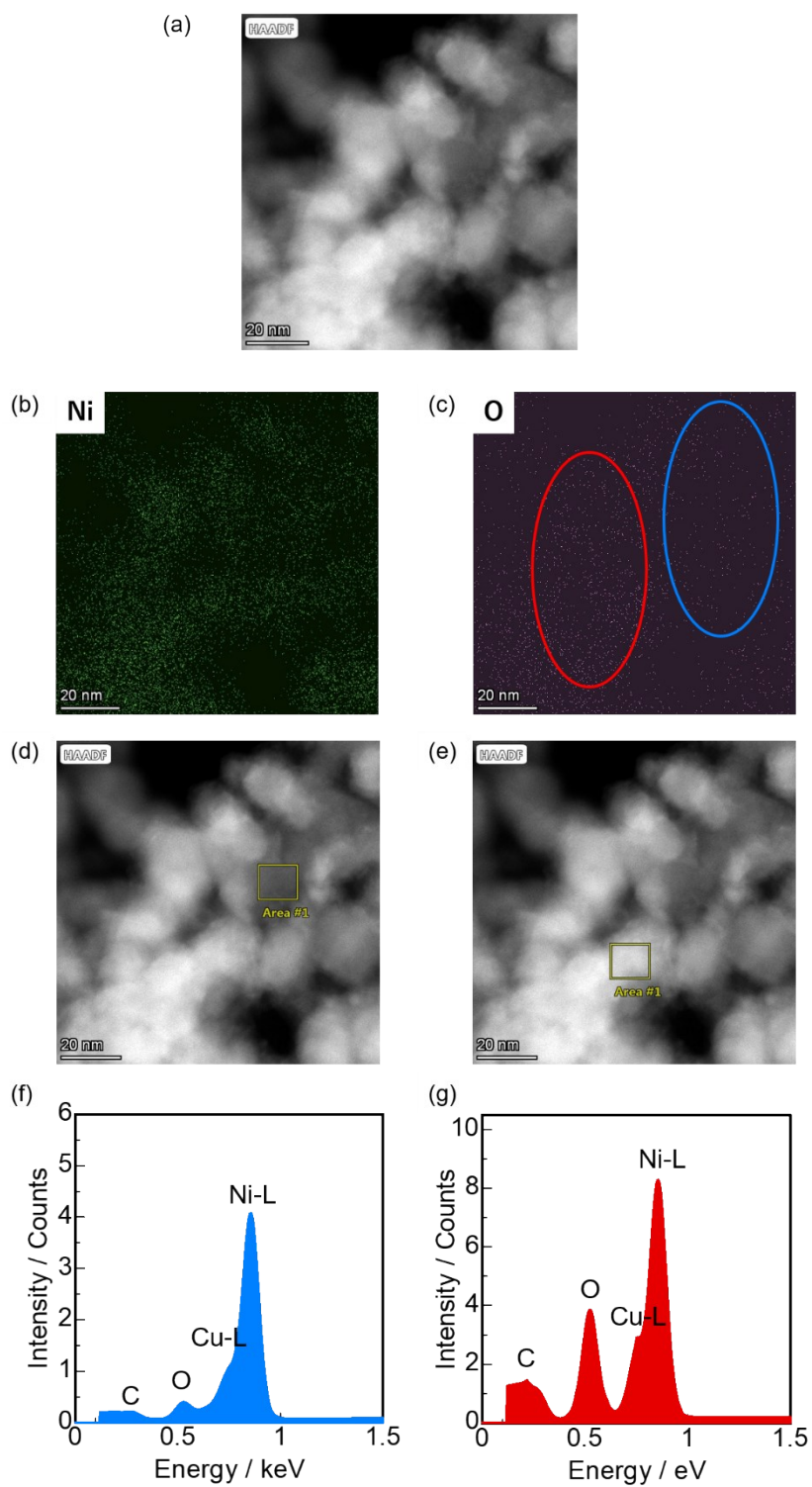


Fig. S3 HAADF-STEM EDS spectra of the freeze-dried Ni/NiO_x.

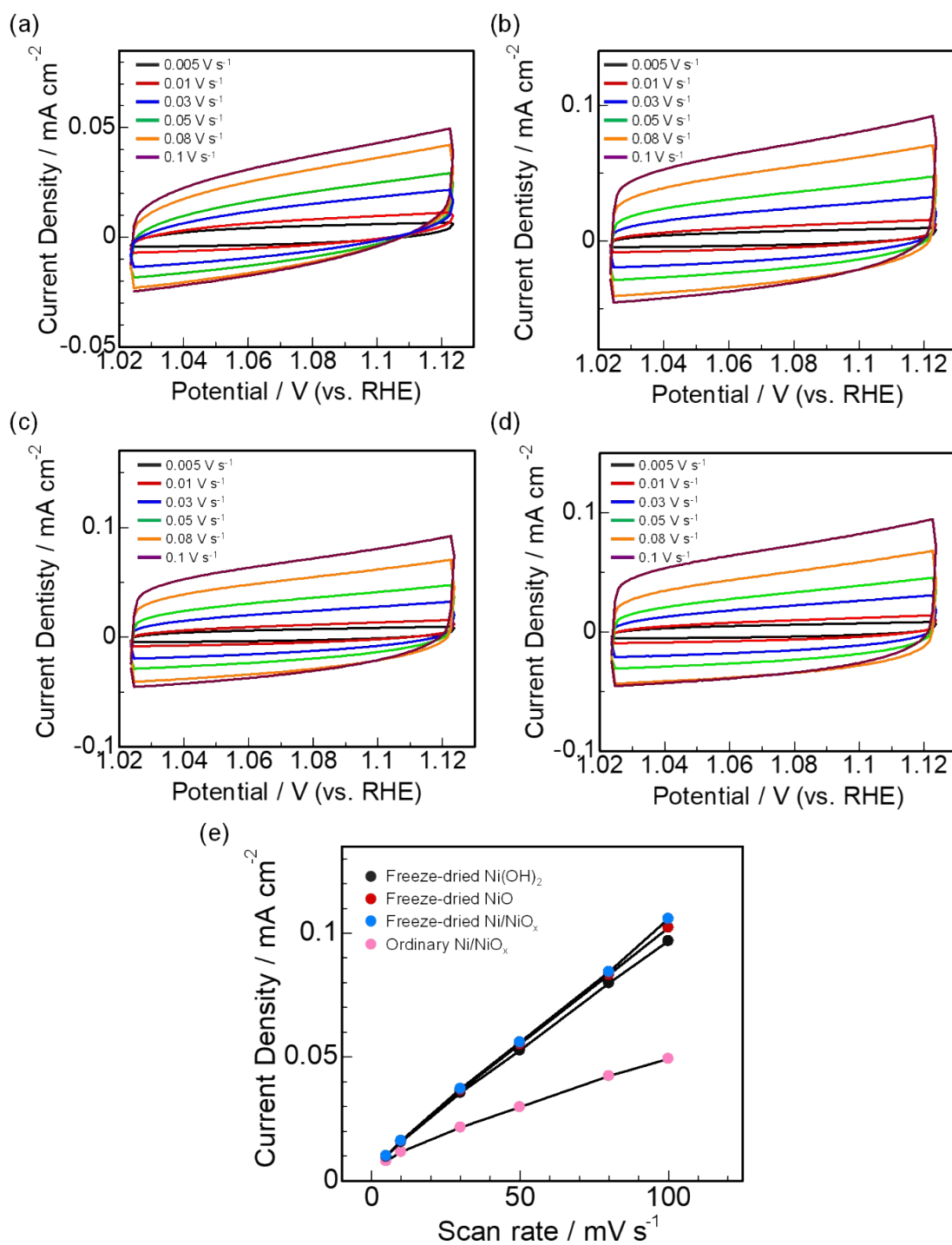


Fig. S4 CV of a) ordinary Ni/NiO_x, b) freeze-dried Ni/NiO_x, c) freeze-dried Ni(OH)₂ and d) freeze-dried NiO collected at different scan rate in 1.0 M KOH solution; e) Calculated double-layer capacitance (C_{dl}) of each sample.

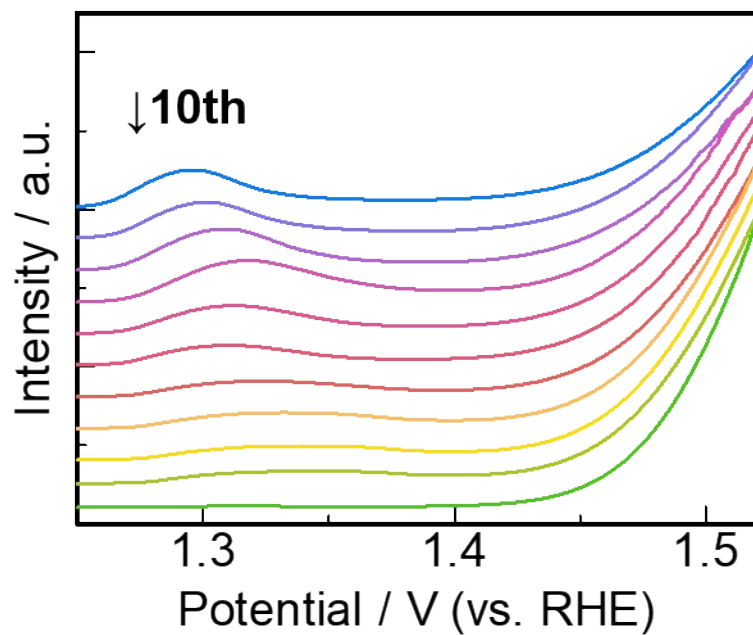


Fig. S5 The OER curves of Freeze-dried Ni/NiO_x between 1st and 100th.

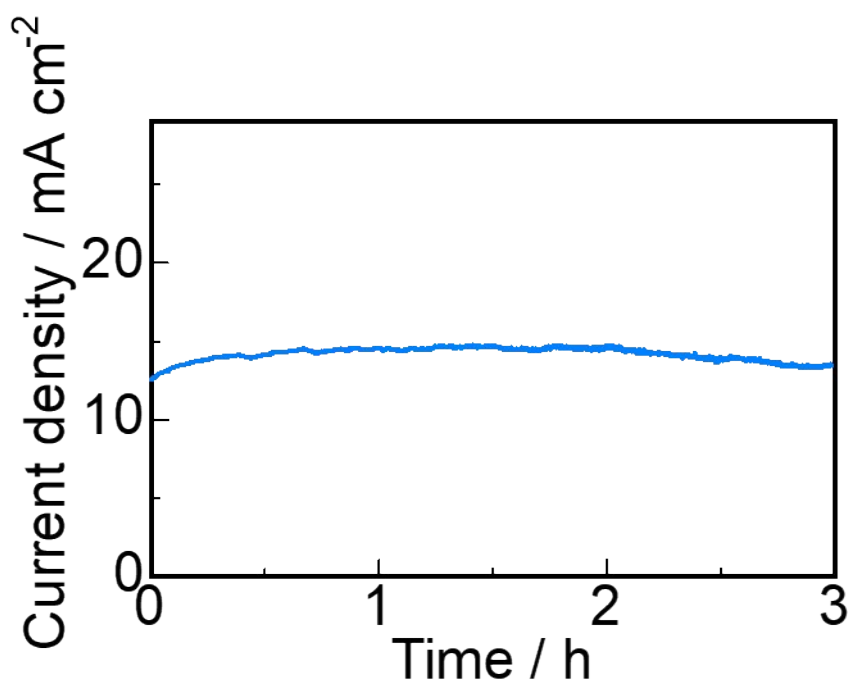


Fig. S6 The chronoamperometric response of freeze-dried Ni/NiO_x at 1.5V

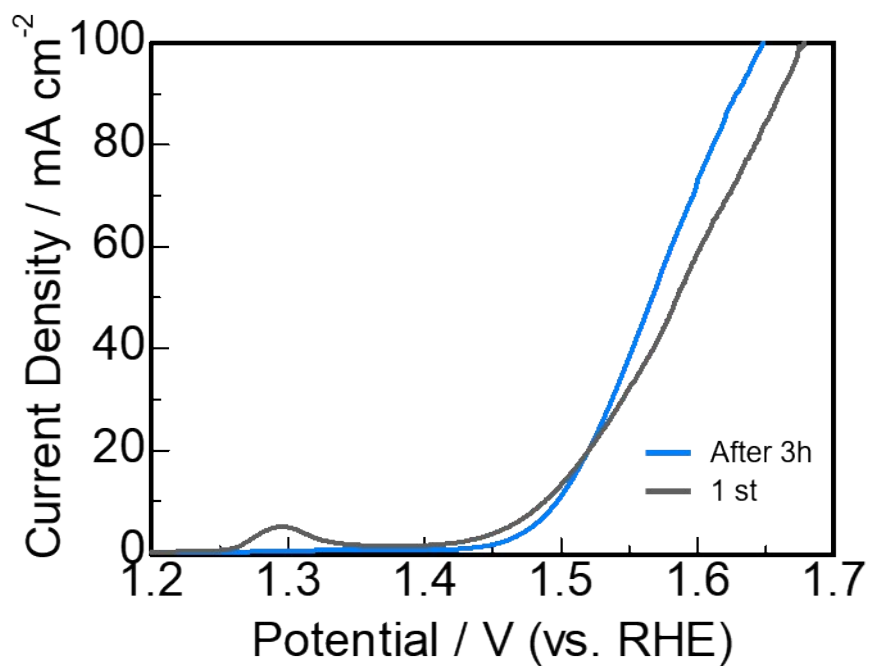


Fig. S7 The OER curves of Freeze-dried Ni/NiO_x after 3h of the chronoamperometric measurement.

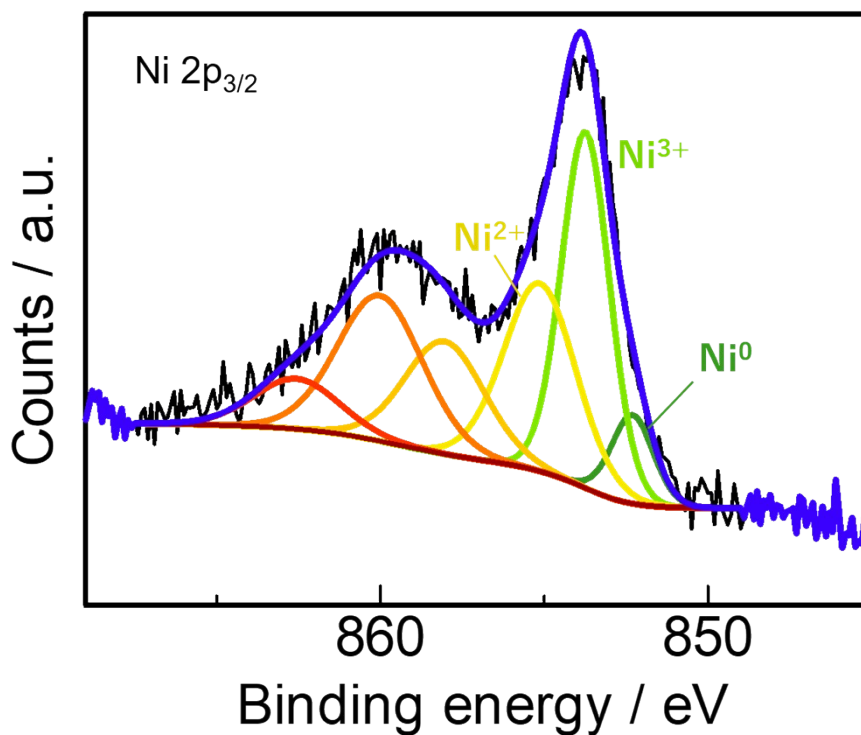


Fig. S8 XPS spectra of Freeze-dried Ni/NiO_x after 100 scans.

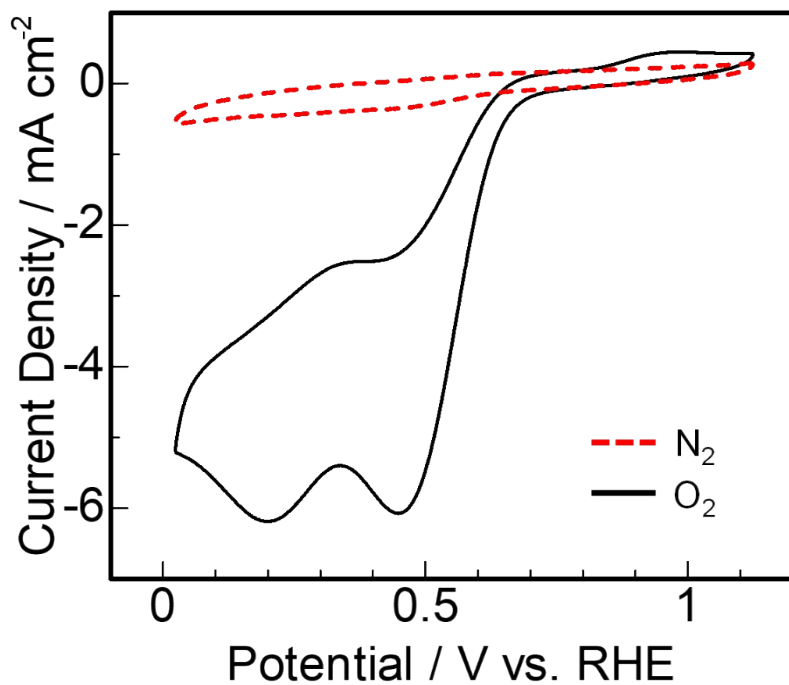


Fig. S9 The CV measurement of freeze-dried Ni/NiO_x under N₂ or O₂.

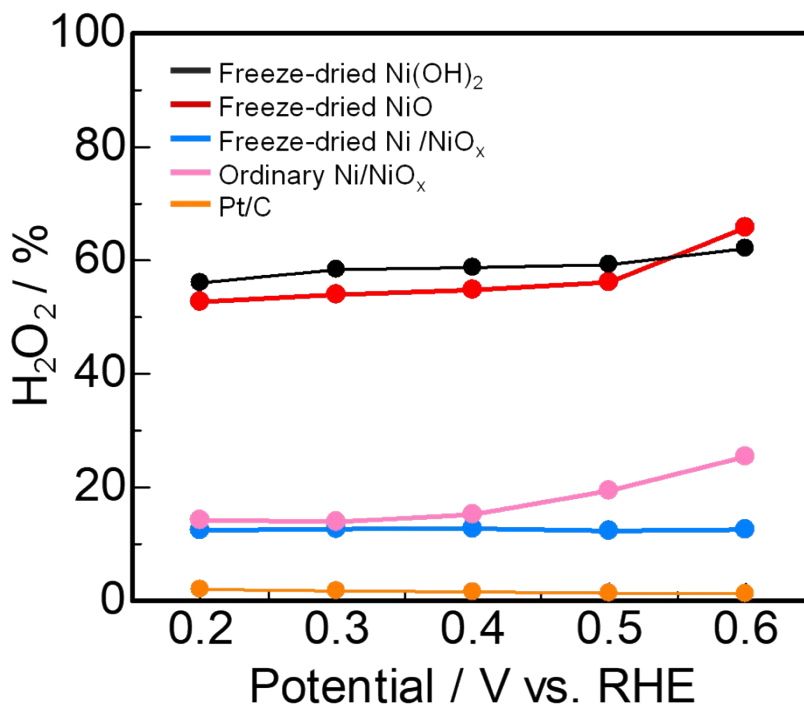


Fig. S10 The yield of hydrogen peroxide.

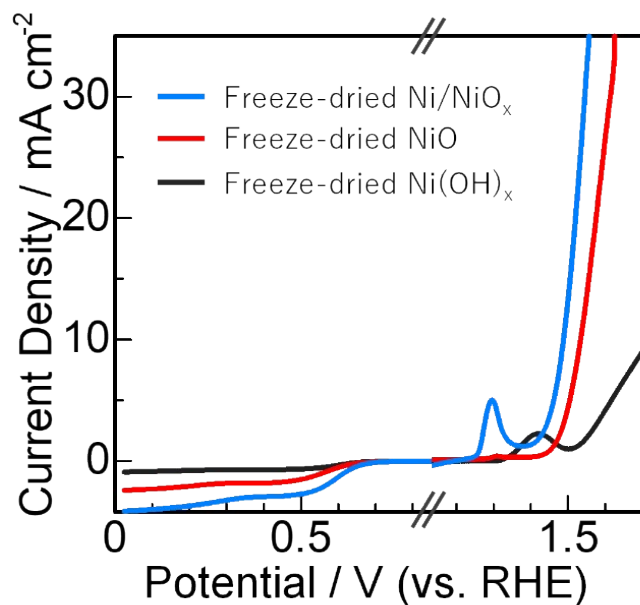


Fig. S11 LSV curves for OER and ORR to evaluate ΔE .

Table S1 Comparison of the OER and ORR activity of freeze-dried Ni/NiO_x with those of Ni based products in reference. Reference numbers belong to the main text.

	Over potential ($E_{i=10}$)	Tafel slope	Half-wave potential ($E_{1/2}$)	Electron transfer number	Electrolyte	Ref. number
Freeze-dried Ni/NiO _x	240	37	0.62	3.8	1M KOH	This work
Freeze-dried NiO	309	50	0.55	3.0	1M KOH	This work
Freeze-dried Ni(OH) ₂	370	35	0.56	2.9	1M KOH	This work
NiO/NF-400	310	54	–	–	1M KOH	[15]
Porous Ni/NiO	260	62	0.75	3.8	0.1M KOH	[22]
Ni/NiO nanosheets	300	71	–	3.3	0.1M KOH	[22]
NiO nanosheets	460	178	–	3.0	0.1M KOH	[22]
NiO _x /Ni	390	80	–	–	1M KOH	[32]
AC-NiO	320	49	–	–	1M KOH	[37]
NiO	360	76	–	–	1M KOH	[37]
Ni/NGr	390	98	0.62	3.7-3.9	0.1M KOH	[38]
Ni/Gr	550	–	–	–	0.1M KOH	[38]
Ni@NiO/N-C NW	390	100	–	–	1M KOH	[39]
Ni-NiO@3DHPG	310	55	–	–	1M KOH	[40]

Reference

15. P. T. Babar, A. C. Lokhande, M. G. Gang, B. S. Pawar, S. M. Pawar, J. H. Kim, *J. Ind. Eng. Chem.*, 2018, **60**, 493-497.
22. P. Liu, J. Ran, B. Xia, S. Xi, D. Gao and J. Wang, *Nano-Micro Lett.*, 2020, **12**, 68.
32. G.-Q. Han, Y.-R. Liu, W.-H. Hu, B. Dong, X. Li, X. Shang, Y.-M. Chai, Y.-Q. Liu and C.-G. Liu, *Appl. Surf. Sci.*, 2015, **359**, 172-176.
37. S. Sekar, D. Y. Kim and S. Lee, *Nanomaterials (Basel)*, 2020, **10**, 1382.
38. S. N. Faisal, E. Haque, N. Noorbehesht, H. Liu, M. M. Islam, L. Shabnam, A. K. Roy, E. Pourazadi, M. S. Islam, A. T. Harris and A. I. Minett, *Sustain. Energy Fuels*, 2018, **2**, 2081-2089.
39. A. Xie, J. Zhang, X. Tao, J. Zhang, B. Wei, W. Peng, Y. Tao and S. Luo, *Electrochimica Acta*, 2019, **324**, 134814.
40. N. Ullah, W. Zhao, X. Lu, C. J. Oluigbo, S. A. Shah, M. Zhang, J. Xie and Y. Xu, *Electrochimica Acta*, 2019, **298**, 163-171.